Principles of optical design of the SM beamline at the CLS

K. Kaznacheyev*[1], I. Blomqvist[1], E. Hallin[1]; S. Urquhart[2]; D. Loken[3]; T. Tyliszczak[4], T. Warwick[4], A.P. Hitchcock[5],

1. CLS, U of Saskatchewan, Saskatoon SK S7N OX4, Canada
2. Chemistry Department, U. of Saskatchewan, Saskatoon SK S7N 5C9, Canada
3. FSDG, Saskatoon SK S7L 6H5, Canada
4. ALS, LBNL, Berkeley CA 94720, USA
5. Brockhouse Institute for Materials Research, McMaster Univ., Hamilton ON L8S 4M1, Canada.

Abstract. The spectromicroscopy beamline (SM) at the Canadian Light Source (CLS) will provide 100 – 2000 eV photons in a high brightness, high flux, medium resolution and small spot size beam. The beamline consists of an advanced elliptically polarized undulator (EPU) source and a novel entrance slit-less plane grating monochromator which feeds two branch lines, one optimized for scanning transmission X-ray microscopy (STXM), the other for X-ray photoemission electron microscopy (X-PEEM). This article outlines the beamline design strategy, and discusses the design optimization relative to the requirements for state-of-the-art STXM and X-PEEM.

DESIGN OBJECTIVES AND CONSTRAINTS

Development of third generation SR sources, enhanced quality soft x-ray optics, and advances in beamline design have lead to the construction of several successful spectromicroscopy (SM) facilities around the world [1]. The SM facility at the Canadian Light Source (CLS), a dedicated soft x-ray beamline and associated scanning transmission x-ray microscope (STXM) and x-ray photoemission electron microscope (X-PEEM), will begin operation in 2004. Here we describe the design principles and solutions adopted to optimize the beamline for these two microscopies.

There is a substantial difference in image formation for these two techniques. In STXM, the source is de-magnified by a Fresnel zone plate (FZP) and the ultimate spatial resolution is defined by the outmost zone width, or ~30nm at current stage of FZP fabrication [2]. To keep such ultimate spot size, the phase accepted by FZP needs to be limited to a single diffraction mode or λ (wavelength of incoming radiation) [3]. As this phase space is much smaller than the emittance of existed SR sources, reduced horizontal phase acceptance can be traded for energy resolving power and overall simplicity. Following the design of the X1A spectromicroscopy beamline at the National Synchrotron Light Source (NSLS), the horizontal dispersing spherical grating monochromator has proved to be a successful choice for several STXM [3-5]. In PEEM, the image is formed by magnified projection of low energy photoelectrons with electrostatic or magnetic electron lenses and recorded with a CCD camera. The dominant chromatic aberrations reduce spatial resolution for most PEEM to ~50 nm in the soft x-ray regime. When this spatial resolution is matched to a megapixel high sensitivity CCD the field of view is of order 30-50 μm. Such moderate spot size can be obtained without any phase (source emittance) loss. The figure of merit analysis of different optical schemes was performed by Weiss et al [6] who concluded that a collimated plane grating monochromator is the optimal choice and further, that it allows further beam size reduction if needed .

To find the optical scheme which best suits both experiments we compared two design concepts, namely a horizontally dispersed spherical grating monochromator (HD-SGM) and a collimated plane grating monochromator with vertical dispersion (PGM) with primary design goal for highest possible on-sample flux in each microscope, with a resolving power exceeding 3000 and covering the energy range 250-2000eV. The results of the comparison follow by a brief presentation of the optical properties of the PGM-based beamline, which was chosen as a best compromise.

The ID10 sector was allocated for the CLS-SM facility, which limits the total length of the beamline to 37m. The lattice parameters (β_x=8.5m, β_y=4.6m, η_x=0.15m, for ε_x=18nmrad and assuming 0.2% coupling as projected for 2008 operation) result in electron beam size (FWHM) Δx=990μ and Δy=30μ [7]. Chiral molecules, magnetic ordering, sample texture and film orientation are among the scientific topics to be studied so full polarization control

CP705, *Synchrotron Radiation Instrumentation: Eighth International Conference,* edited by T. Warwick et al.

TABLE 1. The basic properties of SM EPU assuming 15mm close gap and CLS e-beam parameters as of 2008.

Phase	Effective Horizontal Flux Density (T)	Effective Vertical Flux Density (T)	Photon Energy (eV)	Brightness (ph/s/0.1%bw/ $mm^2/mrad^2$)	Emitting Angle (FWHM, μrad)	On axis Power Density ($kW/mrad^2$)	Total Emitted Power (kW)
Planar	-	0.742	73.4	$4.6*10^{17}$	250	5.7	2.2
Circular	0.492	0.492	82.9	$5.4*10^{18}$	225	0.03	1.9
Vertical	0.652	-	91.7	$6.0*10^{17}$	210	5.0	1.7
45°	0.348	0.348	153.3	$1.1*10^{17}$	170	7.4	1.9

over the undulator properties is required. An elliptically polarized undulator (EPU) based on the original Apple II design [8] with 75mm period is chosen as a compromise of intensity, photon energy range (in first harmonic, it covers L-edges of all 3d elements in circular mode), and a "manageable" power load. The overall EPU parameters are summed in Table 1. It not only covers the 250-2000 eV range, but also is capable of extended operation from 100 to 4000eV with acceptable performance.

The source almost matches the STXM experiment for the whole energy range in the vertical direction but, depending on the energy, STXM can take only 1/4 to 1/30 of the horizontal emittance. There were recently several publications on coherence preservation across the beam, and even a very exciting proposal to build a slit less STXM [9]. We follow a more conservative approach and require a pinhole, or an exit slit in our case, to serve as a spatial filter, limited the phase space seen by FZP to a single diffraction mode. We further assumed that the FZP size shall be 200 μm in diameter, which is an achievable compromise between fabrication ability and desire to have a long focal distance (~ 2mm for carbon K edge). We also add a factor of two overfilling for FZP illumination to reduce possible noise due to angular mis-steering or beam wiggling. The spot size for the PEEM experiment shall be of the order of 30-50μ on a plate inclined at 15° to the beam.

COMPARISON OF HD SGM AND PGM OPTICAL SCHEMES

A horizontally dispersing SGM line is optimized for STXM (Fig.1(a)). The first toroid-shaped mirror deviates the beam by 4° inboard and focuses the source horizontally onto an entrance slit and vertically onto the exit slit. To preserve a reasonable flux at 2keV, SGM including angle is set to 176°. For the moderate grating size (~150mm) at least two gratings (250, 500 l/mm) are needed to cover the 200-2000eV energy range. The vertical demagnification of the first mirror is close to 1:1, and so the requirement to keep FZP overfilled by a factor of two leads to a ZP to exit slit distance of ~2 m. This distance dictates the scaling law for the exit slit opening: $\Delta x=\Delta y\sim\lambda*L(2m)/D(200\mu)$. To match such slit to R>3000 resolving power, the exit arm of SGM needs to be ~6.8 m and the entrance arm ~3.7 m. The last step is a choice of the toroidal mirror to entrance slit distance. A short distance favors PEEM, although for higher that 3:1 demagnification, aberration might be significant, and so a 5 m exit arm is chosen. To separate the PEEM and STXM experimental chambers, a flip geometry was suggested and the PEEM branch features an additional refocusing stage.

The PGM-based design (Fig.1(b)) is based on that of Follath and Senf [10]. The M1 mirror has a sagittal cylinder shape. It deflects the beam horizontally and produces light, almost parallel in vertical direction. The variable angle PGM has a vertical dispersion plane, and, as it is illuminated with collimated light, a wide range of grating magnification may be used (as defined by the c_{ff} parameter, $c_{ff}=\cos\beta/\cos\alpha$, where α-incident angle, β- diffraction angle). Although one grating is enough to cover the whole energy range, two (assumed here as 250/mm optimized for low energy and 1250/mm for high) gives a better performance. After the PGM the beam splits into two branches. The M3PEEM movable mirror deflects the beam toward a short exit arm PEEM branch, while a stationary M3STXM mirror redirects the light into a long arm STXM branch, if M3PEEM is retracted. Both mirrors have toroidal shape and focus light on the exit slits in both vertical and horizontal planes. The separation between the M1 mirror, the PGM scanning unit, and the refocusing mirrors is kept to a minimum and determined mostly by

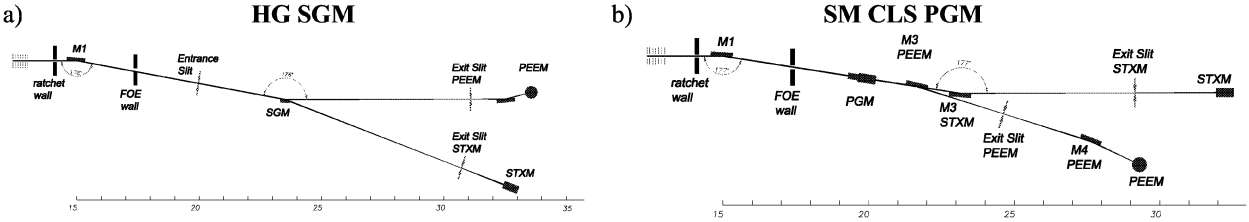

FIGURE 1. Schematic views of the beamline layout: (a) top view of the HD SGM and (b) SM CLS PGM.

convenience (in order to place the PGM outside of the radiation shielded first optical enclosure), and engineering needs. As in the case of the SGM design, a short exit arm (3m) favors PEEM branch and provides a needed compression of the horizontal beam size, while a long arm (6m) better matches STXM. There is a substantial difference to note between the PGM and SGM designs. In the PGM design, the trade-off for the two techniques - optimal angular match for STXM versus intensity preservation for PEEM - happens at the exit slit and so can be optimized independently. By contrast, in the SGM design the entrance slit (which also determines the resolving power) plays this role and once a value has been chosen, it stays the same for both branches. There is an additional demagnification mirror (ellipsoid with 3:1 ratio) for the PEEM branch to produce a small spot matched to the nominal field of view.

The results of the ray tracing analysis of the SGM design (Fig.2a) show that, due to the limited horizontal acceptance, the STXM branch is not affected by defocusing and the main contribution comes from the exit and entrance slits, scaled to keep a single diffraction mode. In contrast, the PEEM branch requires a translational stage for the exit slit to maintain adequate energy resolving power. For the PGM, the optical performance depends both on photon energy and grating magnification. The 2D image plots have a linear energy scale on the vertical axis and a logarithmic c_{ff} scale (from c_{ff}~1/5 (negative order) to c_{ff}~5 (positive order , source is de-magnified)). Due to the mechanical limits, (c_{ff}, E) space is restricted by the total plane mirror deflection angle of 170-178^o and grating diffraction angle to 80-89^o. The energy resolution for the PGM STXM branch in a single diffraction mode is shown in Fig.2a.

The on-sample intensity was calculated analytically by multiplying the brightness propagation by the accepted phase space. The optical element reflectivity and grating efficiency (lamella grating in scalar approximation) are taken into account, as well as the transmission of the two Si_3N_4 membranes in the STXM branch. The ZP efficiency is assumed constant at 5%. To simulate the effect of mirror imperfections a 25% brightness dilution was added for each reflection. The effect of the PEEM refocusing stage and optical aberrations are neglected. In the SGM STXM line at single energy (chosen here as 300eV and 250 l/mm grating) the diffraction limited brightness of the source can be fully preserved and results in a maximum counting rate. Overfilling (not accounted here) and small variation in EPU emitting angle with energy reduce it, but not substantially. A more drastic penalty occurs if the ZP or source parameters are changed. The SGM PEEM branch, even with movable exit slit, has a penalty due to entrance slit transmission, which restricts the horizontal phase acceptance to 1-10%. It also has a problem similar to that for the STXM branch, where , if high resolution is desired, the intensity drops drastically.

An optical scheme similar to PGM PEEM branch was extensively discussed in [6]. It has excellent optical properties, with an on-sample intensity higher by x3 (low energy) to x15 (high energy) than that of an SGM beamline and also features flexibility for further optimization of higher order suppression or high energy resolution. The STXM branch line on the PGM performs lower (by a factor of ~5), than that of the SGM because of two additional loss factors: (a) two more optical surfaces and (b) an additional phase dilution in the vertical direction, especially in positive order. The resulted loss can be partially recovered if the PGM operation is extended into the negative order (c_{ff}<1). In this case, ZP overfilling in the vertical direction is kept at minimum for low energy negative order, but needs to be switched to the positive order at high energy.

As detector efficiency, sample transmission and FZP phase acceptance increases for higher energy light, high order suppression is an important factor. SGM high order filtering is rather poor (Fig.2c), and an additional fixed angle double bounced mirror system has been used to keep it reasonable [3]. If such mirror filter is added, the on-sample STXM intensity for SGM and PGM-based schemes become close, and other factors should be considered.

The power load comparison is performed for the EPU fundamental at ~250 eV with in-plane polarization. At the highest anticipated CLS current (500 mA), the EPU emits ~500 W with a moderate power density of 2.7kW/mrad^2. For the SGM line, the first mirror with a grazing angle 2^o absorbs ~160W with a maximum power load 0.3 W/mm^2 for accepting a solid angle twice that of the EPU central cone. About 10W is absorbed by the entrance slit and ~1.5W by the grating. The power density (Fig.2d) is rather low both due to the entrance slit transmission and shallow incidence angle of the grating at 250eV. The grating deformation is negligible, although the figure accuracy requirement is still high. For the PGM beamline, the first cylindrical mirror has a similar load (total power absorbed 120 W, density 0.2W/mm^2). For 250eV light the PGM plane mirror has a rather steep angle, and so both the total power ~45W and the absorbed power density of 90mW/mm^2 are rather high (Fig.2d). As a result of such high-energy cutoff, the grating (~3W total; 1.5mW/mm^2) and toroidal mirrors (3.5W; 4mW/mm^2 if at zero order) are safe. A careful cooling design is needed to avoid optical performance degradation, especially for the plane mirror of the PGM. Numerical analysis shows that, for Si mirror with internal water cooled channels 1(w)*5(h)mm, placed 1.5mm beneath the optical surface, the resulted mirror deformation is approximately proportional to the power density and will be ~0.6μrad in the above case. For Glidcop, the resolving power will be limited to 3000 for negative order, but can be quickly recovered if high de-magnification (c_{ff} value) will be used. Note, that an extended

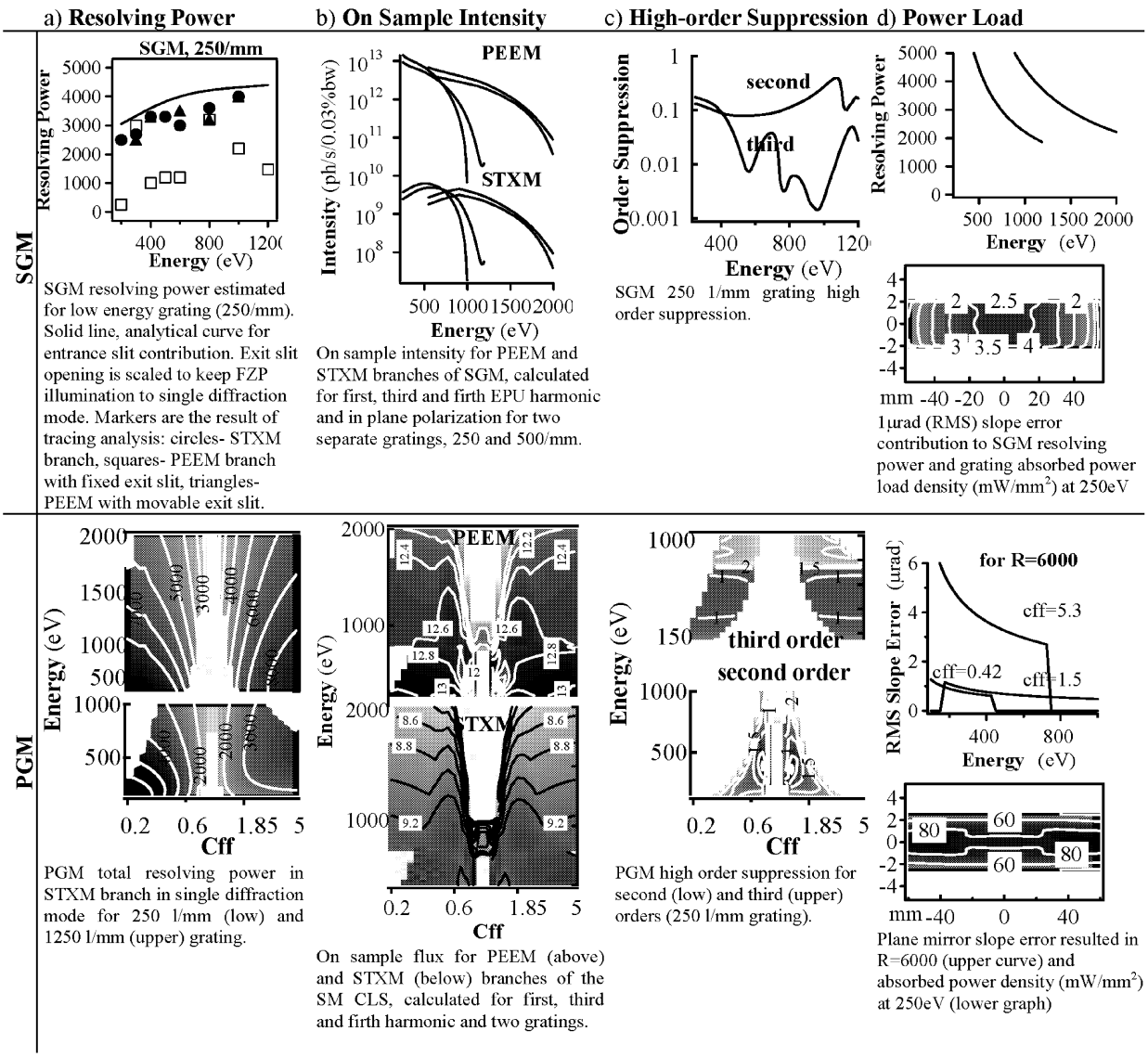

SGM resolving power estimated for low energy grating (250/mm). Solid line, analytical curve for entrance slit contribution. Exit slit opening is scaled to keep FZP illumination to single diffraction mode. Markers are the result of tracing analysis: circles- STXM branch, squares- PEEM branch with fixed exit slit, triangles- PEEM with movable exit slit.

On sample intensity for PEEM and STXM branches of SGM, calculated for first, third and firth EPU harmonic and in plane polarization for two separate gratings, 250 and 500/mm.

SGM 250 1/mm grating high order suppression.

1μrad (RMS) slope error contribution to SGM resolving power and grating absorbed power load density (mW/mm^2) at 250eV

PGM total resolving power in STXM branch in single diffraction mode for 250 l/mm (low) and 1250 l/mm (upper) grating.

On sample flux for PEEM (above) and STXM (below) branches of the SM CLS, calculated for first, third and firth harmonic and two gratings.

PGM high order suppression for second (low) and third (upper) orders (250 l/mm grating).

Plane mirror slope error resulted in R=6000 (upper curve) and absorbed power density (mW/mm^2) at 250eV (lower graph)

FIGURE 2. Cross comparison of optical properties for HD SGM and infinity corrected PGM.

energy range of EPU (till 100eV) does not drastically change these numbers. For instance, if the EPU fundamental is tuned to 95eV, the emitted power triples. Most of it will still be filtered out by the M1 mirror and results in less than 10% absorbed power increase for the plane mirror of PGM and so will result in a similar optical performance. In contrast, tangential deformation of the SGM toroidal mirror will directly result in brightness loss and degrade the STXM performance.

The results of the tracing analysis of PGM line are shown in Fig.3. Toroidal refocusing mirrors, although having noticeable astigmatic aberrations, do not spoil optical performance and the resolving power up to 10,000 can be reached. The e-beam movement results in an energy calibration shift, but it is small and might be further reduced if high c_{ff} parameter is chosen. The PEEM spot size stay at 50 μm even if a toroidal refocusing stage is used. For STXM, there will be an additional phase cut in the horizontal direction at the exit slit, so the slit will always be overfilled and so any beam wiggling shall not lead to noisy STXM images.

Based on the cross comparison outlined above, we chose an infinity corrected slit less PGM for the CLS-SM beamline. The following are the main arguments, which support our choice:

- The entrance slit-less collimated PGM met all SM requirements and would be an universal SM facility, which serves in a rather good way STXM and in an excellent fashion PEEM or a similar experiment.

- It provides great flexibility and operational choice between optimization for (a) high intensity, (b) high order suppression and (c) high energy resolution. It also provides an adequate margin of safety for the stability and the size of the e-beam.
- Power load management, although a challenge, is viable.
- The PGM has a solid performance even for an extended range of operation (100-2500eV). The PGM optical scheme has the flexibility to accept two EPU beams with alternate polarization. The performance does not drastically degrade in such mode [11].
- The space separation between the X-PEEM and STXM experimental areas is reasonable
- One monochromator which serves both branches is a cost effective solution.

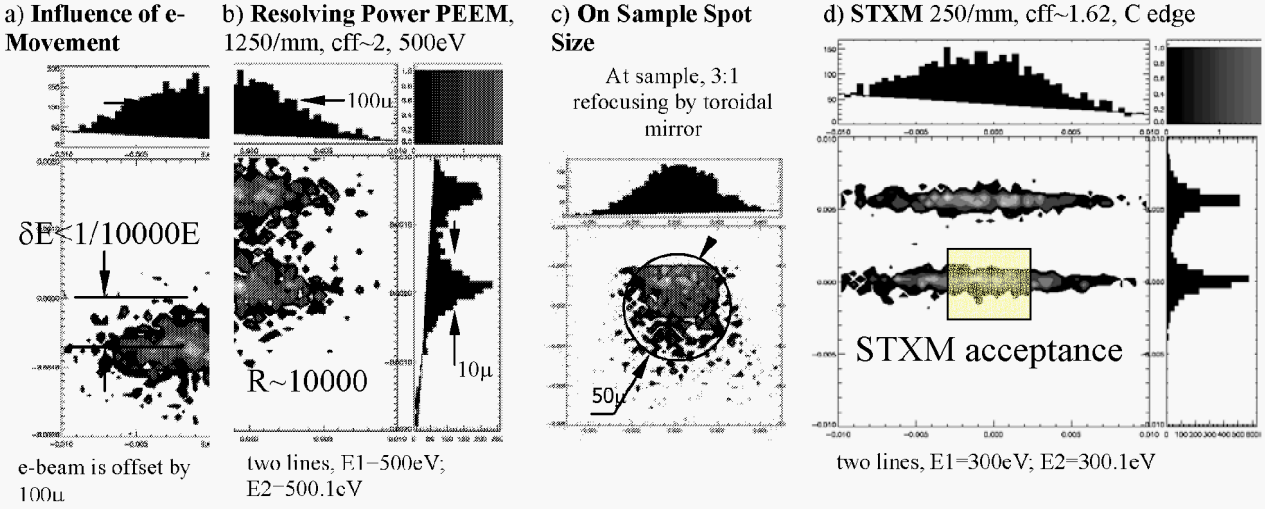

FIGURE 3. Tracing analysis of PGM beamline.

ACKNOWLEDGEMENTS

The authors thank the ALS and Engineering Divisions of the Lawrence Berkeley National Laboratory for assistance in design and engineering through an ALS-CLS co-development agreement. The CLS is funded by many sources, major ones being the Canada Foundation for Innovation, the provinces of Saskatchewan, Alberta and Ontario, the University of of Saskatchewan, the City of Saskatoon and the National Research Council.

REFERENCES

1. Synchrotron Radiation News v.16, N3 (2003), pp. 3-60.
2. M. Peuker, Appl. Phys. Lett., 78 (2001) 2208
3. B. Winn, H.Ade, C.Buckley, M.Feser, M.Howells, S. Hulbert, C. Jacobsen, K. Kaznacheyev, J.Kirz, A. Osanna, J.Maser, I.McNulty, J.Miao, T.Oversluizen, S.Spector, B.Sullivan, Yu.Wang, S.Wirick, H.Zang, J.Synchrotron Rad., 7(2000), 395-404
4. I. McNulty, A.Khounsary, Y.P.Feng, Y.Qian, J.Barraza, C.Benson, D.Shu, Rev. Sci. Instrum. 67, CD-ROM, (1996).
5. T.Warwick, H.Ade, D.Kilcoyne, M.Kritscher, T.Tylizczak, S.Fakra, A.Hitchcock, P.Hitchcock, H.Padmore, J. Synchrotron Rad., 9 (2002), 254
6. M.R.Weiss, R.Follath, F.Senf, W.Gudat, J.of Electron Spec. and Related Phenom., 101-103 (1999), 1003-1012.
7. L.O.Dallin, D.M.Skopic, E.L.Hallin, and J.C.Bergstrom, AIP Conference Proceedings 521, American Institute of Physics, New York, 1999, p. 391.
8. S.Sasaki, K.Miyata, T.Takada, Jpn.J.Appl.Phys., 31 (1992), L1794
9. U.Wiesemann, J. Thieme, P. Guttmann, B. Niemann, D. Rudolph, G.Schmahl, AIP Conference Proceedings 507, American Institute of Physics, New York, 2000, pp.430-434.
10. R.Follath, and F.Senf, NIM A 390 (1997), pp.388-394.
11. K.J.S.Sawhney, F.Senf, M.Scheer, F.Schafers, J.Bahrdt, A.Gaupp, W.Gudat, NIM A 390 (1997), 395-402.